UDC 629.5.028.7:629.514

Dongsheng QIAO[1]
Binbin LI[2]
Jinping OU[1]

Comparative Analysis on Coupling Effects between an Innovative Deep Draft Platform and Different Mooring Models

Original scientific paper

In global responses analysis for an innovative deep draft multi-spar platform, three different types of the mooring system are considered, namely a catenary, a semi-taut and a taut mooring system. These three types of mooring systems have the same arrangements with similar static restoring force characteristics. In this paper, the platform motions and mooring responses in three different water depths ranging from 500 m to 1500 m are analyzed. The coupling effects between the spar platform and its mooring lines are investigated through a numerical simulation method. Free-decay and three hours simulations under certain sea state conditions in the South China Sea are executed. The specific numerical results and analysis conclusions would be helpful for mooring system selection and motion performance study in the preliminary design.

Keywords: *spar, mooring system, coupled analysis, responses, tension*

Usporedna analiza različitih konfiguracija sidrenog sustava u spregnutom odzivu novog tipa platforme s dubokim gazom

Izvorni znanstveni rad

U analizi globalnog odziva novog tipa platforme s dubokim gazom tj. multi-spar platforme, razmatrana su tri različita tipa sidrenog sustava: sidreni sustav s lančanicama, polu-napeti te zategnuti sidreni sustav. Navedeni sidreni sustavi imaju isti tlocrt te sličnu krutost. U ovom radu, gibanje platforme i odzivi sidrenog sustava analizirani su za dubine mora od 500 do 1500 m.

Sprega između spar platforme i pripadnog sidrenog sustava istražena je kroz numeričku simulaciju.

Provedeni su proračuni slobodnih oscilacija platforme (eng. *free-decay*). Također su provedene simulacije u trajanju od tri sata realnog vremena za određeno stanje na poziciji Južnog kineskog mora. Dobiveni rezultati biti će korisni za odabir sidrenog sustava u preliminarnom projektu.

Ključne riječi: *spar platforma, sidreni sustav, spregnuta analiza, odzivi, vlačna sila*

Authors' addresses (Adrese autora):
[1] *Deepwater Engineering Research Center, Dalian University of Technology*, Dalian, China
Email: qds903@163.com
[2] *Regional Oil & Gas Offshore Center, Bureau Veritas*, Singapore

Received (Primljeno): 2012-04-18
Accepted (Prihvaćeno): 2012-05-25
Open for discussion (Otvoreno za raspravu): 2013-12-31

1 Introduction

In recent years, the application and research of floating platforms are becoming more and more widespread with the exploration of deepwater hydrocarbon resources in deep and ultra-deep waters. The types of floating platforms such as Semi-Submersible Platform, Spar Platform and Floating Production Storage and Offloading (FPSO) need to be positioned through a mooring system when they are working as production platforms. The integrity of production risers depends on the station keeping ability. Now the floating platforms are moving beyond water depths of 2000 m and target a 3000 m range, so the need for efficient station keeping mooring systems increases.

The commonly used mooring systems include three types: catenary, semi-taut and taut. The catenary mooring system is widely applied in practice during these years and is usually made up of a chain, a wire or a combination of them. The catenary mooring system supplies restoring force to the platform depending on the weights of the mooring line. With the increasing water depth, the high weight of the chain becomes one of the restrictions. The representative feature of the catenary mooring system is that parts of the bottom chain keep lying on the seabed when the platform moves. The semi-taut mooring system supplies restoring force to the platform depending on weights and elastic deformation of the mooring line. The taut mooring system supplies restoring force to the platform depending on elastic deformation of the mooring line [1].

Compared with the catenary mooring system, the taut mooring system has some advantages: a small positioning radius which may reduce occupation area of the seabed and interference with other underwater facility; a small length of the mooring line which may reduce economic costs [2, 3]. The taut mooring system usually has a high restoring stiffness which may cause a high mooring line tension, so the safety margin is lower than in the catenary mooring system. The characteristics of the semi-taut mooring system are a combination of those of the catenary and the taut mooring systems.

In the past years, many scholars have revealed that the coupling effects between the floating platform and its mooring system should be considered in predicting their motions [4-6]. A coupled dynamic analysis technique has been developed from a quasi-static approach [7] to a fully coupled dynamic approach [8-12]. In the quasi-static method, the mooring lines are treated as a massless linear or nonlinear spring and the hull responses are calculated as well as the mooring tension from the static mooring load. In the fully coupled dynamic method, the hydrodynamic effect of the mooring lines is particularly considered. Despite this, only a few scholars investigate the impact of different mooring models on the motions of a floating platform. Chen et al. [13] use a quasi-static approach (SMACOS) and a coupled dynamic approach (COUPLE) to calculate motions of a spar and its mooring system in three water depths. Shafieefar and Rezvani [14] present a genetic algorithm to optimize the mooring design of floating platforms. Tong et al. [15] compare the dynamic effect for a semi-submerged platform with a catenary and a taut mooring system. Sun and Wang [16] study the motion performance of deepwater spar platform under equally distributed mooring method and grouped mooring method.

To reveal the coupling effects between a floating platform and different mooring models, and give some suggestions on the mooring system selection in the preliminary design, the analysis of an innovative Deep Draft Multi-Spar (DDMS) platform is presented in this work. Global responses of the spar platform using a catenary, a semi-taut and a taut mooring system in 500 m, 1000 m, 1500 m water depths are calculated. The three different mooring system types have the same arrangements with similar static restoring force characteristics.

2 Description of DDMS platform and environmental conditions

2.1 DDMS platform and mooring system configurations

The DDMS platform concept (shown in Figure 1) combines the advantages and design features of the Truss Spar and SEMI platforms. The DDMS looks like a semi-submersible platform; however the hydrodynamics resembles that of a spar platform. Table 1 summarizes the main characteristics of the DDMS platform. For more information, refer to Li and Ou [17].

Table 1 **Features of DDMS platform**
Tablica 1 **Karakteristike DDMS platforme**

	Value	Unit
Diameter of single spar	12.50	m
Distance between spars	35.50	m
Outer diameter of moonpool	18.00	m
Height of spar	99.60	m
Average draft	151.60	m
Total displacement	68756.00	t
Light ship weight	28926.14	t
Ballast weight	22000	t
Pitch/Roll gyration radius	68.47	m
Center of gravity above keel (KG)	83.57	m
Center of buoyancy above keel (KB)	89.82	m

The mooring system consists of four (4×4) groups as shown in Figure 2. Each mooring line consists of three segments: an upper chain, a middle wire and a bottom chain. Each group in the mooring system is separated by 90-degree spacing and each line in the same group is separated by 5-degree spacing. The three types of the mooring system, i.e. a catenary, a semi-taut and a taut mooring system, are calculated and added to the spar platform.

Figure 1 **DDMS platform**
Slika 1 **DDMS platforma**

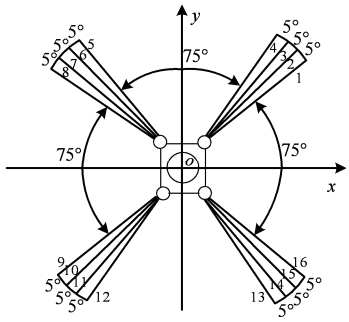

Figure 2 **Mooring system layout**
Slika 2 **Tlocrt sidrenog sustava**

Considering the gravity, tension, and mooring line extension, the piecewise extrapolating method is employed to the static analysis of the multi-component mooring line [18]. Aiming to ensure that the three types of the mooring positioning system have the similar static restoring force characteristics, the arrangement of the three segments in the taut mooring system may not meet the practical application demands of project, but its use in this research is still suitable.

Through the optimization design of the three types of the mooring system, the mooring systems configurations for 500 m, 1000 m, and 1500 m water depths are specified in Table 2. The mooring line properties are shown in Table 3. The representative tension-horizontal displacement characteristic curve of a single mooring line (#1) is plotted in Figure 3. The total horizontal force-horizontal displacement is plotted in Figure 4.

Table 2 **Mooring system configurations**
Tablica 2 **Konfiguracije sidrenog sustava**

Water depth (m)		Length (m)			Pretension (kN)
		Upper chain	Middle wire	Bottom chain	
500	Catenary	100	700	500	1000
	Semi-taut	50	500	275	900
	Taut	300	350	30	825
1000	Catenary	200	1400	1000	2000
	Semi-taut	200	1100	550	1950
	Taut	550	700	60	1650
1500	Catenary	300	2000	1500	3000
	Semi-taut	300	1600	800	2900
	Taut	900	1100	100	2650

Table 3 **Mooring line properties**
Tablica 3 **Karakteristike sidrenih linija**

Item	Chain (K4 studless)	Wire (Sprial strand)
Diameter (m)	0.095	0.095
Weight in water (N/m)	1605.9	356.9
Axial stiffness (N)	6.7681E8	8.3391E8
Breaking stress (N)	9.0444E6	7.8765E6

3 Hydrodynamics and numerical full coupled method

3.1 Hull hydrodynamics

The hard tank and the ballast tank of DDMS are modelled as panel elements, and subsequently the potential flow theory is adopted to calculate the wave hydrodynamic information involving the 1st order wave exciting force, steady wave drift force, frequency-dependent added mass, and radiation damping. The hull panel model is shown in Figure 5.

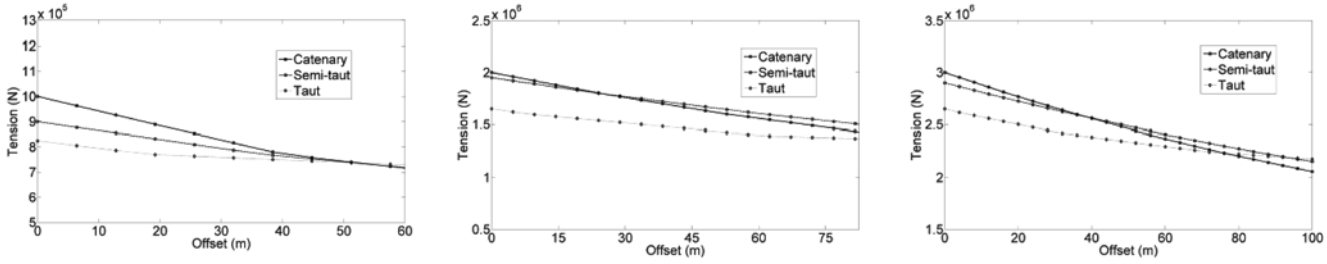

3(a) 500 m 3(b) 1000 m 3(c) 1500 m

Figure 3 **Static offset curve of single mooring line**
Slika 3 **Statički horizontalni pomak jedne sidrene linije**

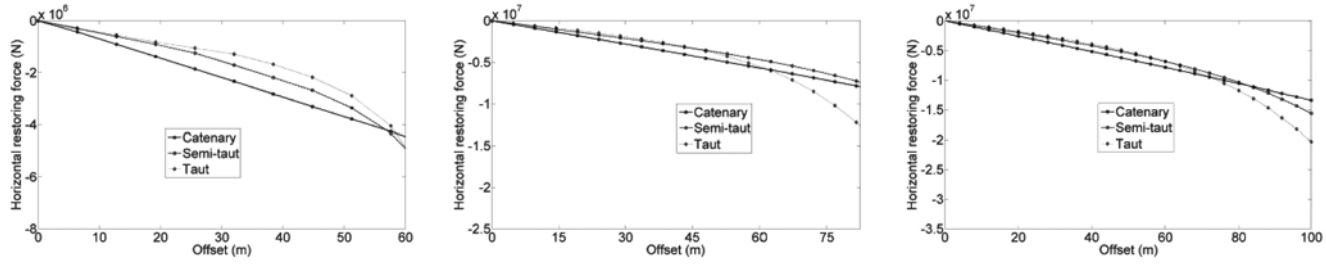

4(a) 500 m 4(b) 1000 m 4(c) 1500 m

Figure 4 **Surge static offset curve of mooring system**
Slika 4 **Uzdužni statički pomak sidrenog sustava**

2.2 Environmental Conditions

The environmental conditions considered include a certain sea state in the South China Sea as listed in Table 4. The mean wind speed, JONSWAP wave spectrum, and uniform current along water depth are used in the numerical simulation. The wind, wave, and current are assumed collinear. The environmental heading is assumed to be from X-axis as shown in Figure 2.

Table 4 **Environmental conditions**
Tablica 4 **Okolišni uvjeti**

Item		Value
Wind speed (m/s)		23.15
Wave	Significant wave height (m)	6.0
	Peak period (s)	12.2
Current speed (m/s)		0.93

Figure 5 **Coupled model**
Slika 5 **Spregnuti model**

Since the 1st order hydrodynamic problem of a floating body can be separated into 2 components i.e. the forces and moments

on the body due to incident regular waves as well as the forces and moments on the body when the structure is forced to oscillate with the wave excitation frequency. Thus, the total 1st order velocity potential can be determined [19]:

$$\phi^{(1)}(X,t) = [(\phi_I + \phi_D) + \sum_{j=1}^{6} \phi_j x_j]\mathrm{e}^{-i\omega t} \tag{1}$$

where ϕ_I, ϕ_D, ϕ_D, x_j, X and ω are incident wave potential, diffraction wave potential, potential due to jth motion, jth motion, reference axes and wave frequency respectively. The last item of square bracket at the right hand side of formula (1) reflects the radiation effects and furthermore determines the added mass and radiation damping subsequently. The unknown potentials appearing in formula (1) are calculated by using Green's functions with the required boundary conditions on the surfaces. Finally, the 1st order wave exciting forces and moments are obtained by integrating the pressure over the wetted surface of the body [19]:

$$F_j^{(1)} = \mathrm{Re}[i\int_{S_B} \rho\omega e^{-i\omega t}(\phi_I + \phi_D)n_j \mathrm{d}S] \qquad (j = 1,...,6) \tag{2}$$

where ρ, n_j and S_B represent the water density, generalized surface normal for jth direction and wetted body of the structure in calm water respectively; j = 1,...,6 denote the 6 degrees of freedom, i.e. surge, sway, heave, roll, pitch and yaw. As described above, the forces when the structure is forced to oscillate with the wave excitation frequency can be expressed as a summation of real and imaginary parts [19]:

$$F_{ji}^{(1)} = -\mathrm{Re}[-\frac{\rho}{\omega}\int_{S_B} \phi_i n_j \mathrm{d}S]\ddot{x}_i - \mathrm{Im}[\rho\int_{S_B} \phi_i n_j \mathrm{d}S]\dot{x}_i \qquad (i,j = 1,...,6) \tag{3}$$

and furthermore the above formula is simplified [19]:

$$F_{ji}^{(1)} = -A_{ji}\ddot{x}_i - B_{ji}\dot{x}_i \qquad (i,j = 1,...,6) \tag{4}$$

where A_{ji}, B_{ji}, $\dot{x}_i$ and $\ddot{x}_i$ are added mass coefficient, radiation damping coefficient, velocity and acceleration of ith motion; $F_{ji}^{(1)}$ represents the force in jth direction due to the ith motion.

Once the 1st order transfer functions are obtained, wave force in time domain under irregular wave can be obtained as below [20, 21]:

$$F^{(1)} = \sum_{i=1}^{N} T^{(1)} A_i \cos(\omega_i t + \varepsilon_i) \tag{5}$$

where $T^{(1)}$ and ε_i are transfer function and random phase within $0 \sim 2\pi$. A_i denotes the wave amplitude component and is determined by the formula below [20, 21]:

$$A_i = \sqrt{2S_\eta(\omega_i)\Delta\omega} \tag{6}$$

where $S_\eta(\omega_i)$ expresses the wave spectrum.

The radiation damping in time domain is achieved by introducing the retardation function and the platform velocity with convolution integral approach. R is the retardation function defined as below [20, 21]:

$$R(t) = \frac{2}{\pi}\int_0^\infty B_{ji}(\omega)\cos\omega t \mathrm{d}\omega \tag{7}$$

The added mass can be treated as a constant value at infinite frequency [20, 21]:

$$a_{ji} = A_{ji}(\omega') + \frac{1}{\omega'}\int_0^\infty R(t)\sin\omega' t \mathrm{d}t \tag{8}$$

where ω' is an arbitrary frequency.

The 2nd order wave slow drift forces are calculated using the full QTF matrix while discarding the 2nd order sum-frequency forces which contribute almost nothing to the response. Generally, the 2nd order wave slow drift force can be written as below [22]:

$$\begin{aligned} F_{sv}(t) = \sum_{i=1}^{N}\sum_{j=1}^{N}\Big\{ & T_{ij}^{ic}\cos[(\omega_j - \omega_i)t + (\varepsilon_j - \varepsilon_i)] + \\ & + T_{ij}^{is}\sin[(\omega_j - \omega_i)t + (\varepsilon_j - \varepsilon_i)]\Big\} \end{aligned} \tag{9}$$

where T_{ij}^{ic} and T_{ij}^{is} denote the in-phase and out-of-phase components of 2nd order transfer functions; ω_i, ω_j, ε_i, ε_j and N are the frequencies of each pair of wave components, random phase angles corresponding to the wave components and number of wave components. According to the application of full QTF, T_{ij}^{ic} and T_{ij}^{is} are both necessity to be calculated by considering variety of contribution, e.g. 1st and 2nd order effects as follows [22]:

$$\begin{aligned} T_{ij}^{ic} = & -\oint_\Gamma \frac{1}{4}\rho g\zeta_i\zeta_j\cos(\varepsilon_i - \varepsilon_j)\vec{n}\mathrm{d}l + \iint_{S_B}\frac{1}{4}\rho\left|\nabla\phi_i\right|\left|\nabla\phi_j\right|\vec{n}\mathrm{d}S + \\ & + \iint_{S_B}\frac{1}{2}\rho(X_i\nabla\frac{\partial\phi_j}{\partial t})\vec{n}\mathrm{d}S + MR_i\ddot{X}g_j + \iint_{S_B}\rho\frac{\partial\boldsymbol{\phi}^{(2)}}{\partial t}\vec{n}\mathrm{d}S \end{aligned} \tag{10}$$

$$\begin{aligned} T_{ij}^{is} = & -\oint_\Gamma \frac{1}{4}\rho g\zeta_i\zeta_j\sin(\varepsilon_i - \varepsilon_j)\vec{n}\mathrm{d}l + \iint_{S_B}\frac{1}{4}\rho\left|\nabla\phi_i\right|\left|\nabla\phi_j\right|\vec{n}\mathrm{d}S + \\ & + \iint_{S_B}\frac{1}{2}\rho(X_i\nabla\frac{\partial\phi_j}{\partial t})\vec{n}\mathrm{d}S + MR_i\ddot{X}g_j + \iint_{S_B}\rho\frac{\partial\boldsymbol{\phi}^{(2)}}{\partial t}\vec{n}\mathrm{d}S \end{aligned} \tag{11}$$

where Γ, ζ, X, $\ddot{X}g$, M, R and $\phi^{(2)}$ are the water line along the structure surface, relative wave surface elevation, motion at structure surface, acceleration vector of the centre of gravity, structure mass, rotation matrix and 2nd order potential, respectively. The five items on the right hand side of the terms (6) and (7) reveal the contributions of relative wave elevation by waterline integral, pressure drop due to the first order velocity via the Bernoulli equation, pressure due to product of gradient of the first order pressure and the first order forces, products of the first order angular motions and inertia forces as well as the products of the 2nd order potentials, respectively.

Besides the hard tank and the ballast tank whose hydrodynamics are predicted by potential theory described previously, the middle section, composed of columns, is simulated as elements of Morison type considering the drag, inertial and added mass forces due to its small diameter compared with the wave length. The Morison force for each element is expressed below [23]:

$$F_{Mor} = C_I\rho\frac{\pi D^2 l}{4}\dot{u} - C_a\rho\frac{\pi D^2 l}{4}\ddot{x} + \frac{1}{2}\rho C_d(u - \dot{x})\left|(u - \dot{x})\right|Dl \tag{12}$$

where D, l, C_a, $C_1 = C_a + 1$ and C_d are diameter, length, added mass, initial force and drag coefficients of Morison element; u, $\dot{u}$, $\dot{x}$ and $\ddot{x}$ denote the flow velocity, flow acceleration, element velocity and element acceleration respectively. For the heave plates, due to their extraordinary thin thickness, some special disc elements with no thickness and mass are used to represent the added mass and drag forces [24]:

$$F_P = \frac{8}{3}C_a\rho r^3\ddot{y} + \frac{1}{2}C_d\rho\pi r^2\dot{y}\left|\dot{y}\right| \tag{13}$$

where F_P, r and y express the hydrodynamic force for heave plate, radius of disc and relative vertical displacement. The viscous damping induced by hard tank, significantly limiting the surge response near the natural period in low frequency range, is estimated by employing the Morison drag item.

3.2 Mooring dynamics

The mooring tension generated from the quasi-static method for floating platform is commonly validated to be a non-conservative estimation. Thus, accurate assessing of the tension through dynamic treating is not only important for the above-mentioned hull motion, but also for the reliable design of the mooring lines. The analytical strategy of mooring dynamics in the paper disperses the cable into a certain amount of elements which are calculated in the local axis system and accounting of some nonlinear factors e.g. drag and inertial forces. The element motion equation is as follows [25, 26]:

$$(M_m + M_{ma})\ddot{r} = F_g + F_b + F_d + F_s + (\lambda r')' - (Br'')'' \tag{14}$$

where, M_m, and M_{ma} denote the structural mass, added mass matrixes (6 x 6); $r(s, t)$ is the position vector of the mooring line which is a function of arc length s and time t; $\ddot{r} = \frac{\partial^2 r}{\partial t^2}$ is the acceleration; F_g, F_b, F_d and F_s are gravity force, buoyancy force, drag force, and sea bed reactions vectors (6 x 1) respectively; $\lambda = T - B\kappa^2$ is the effective tension, where T stands for the local tension, and κ stands for the local curvature of the mooring line; B is the bending stiffness. $r' \cdot r' = 1 + 2\frac{T}{EA}$ is the implicit condition, where EA is the elastic stiffness of the mooring line. In fact the equation above has 6 degrees of freedom for 2 nodes of an element, and each node has three degrees including one inline and two normal directions.

3.3 Coupled Analysis

In time domain simulation, the motion solution for the hull and mooring during a time history are fully coupled. The forces and displacements at the fairlead are the same, and the tension for the mooring line and the motion of the hull are considered to be mutually interactive where the mooring line affects the hull motion. In this case, the element length selection for the hull panel is based on the research by Garrett et al. [21], and each mooring line is divided into 50 elements which ensure adequate calculation precision and computational efficiency throughout the tests.

The coupled equations for the hull and the mooring systems are solved in the time domain using the *Netwark* – β method [27]. At each time step, the positions, velocity and acceleration are predicted firstly through the data at the previous time step, and then the correctors are calculated based on the coupled motion equations. This iteration is repeated until the difference between the two correctors is less than the error tolerance, and then the simulation moves to the next time step.

4 Numerical simulation and results analysis

4.1 Natural periods

The natural periods for the three types of the mooring system in 500 m, 1000 m, and 1500 m water depths are obtained from free decay tests in calm water according to the first six periods. The initial amplitudes for surge, heave and pitch respectively are 10 m, 2 m and 10 degrees [28]. The natural periods derived from free decay simulations in calm water are summarized in Table 5. Figure 6 shows the surge, heave and pitch free decay test results in 1500 m water depth, and the ones in 500 m and 1000 m water depths are omitted for the sake of conciseness.

According to Table 5, the natural periods of surge for the taut mooring system are longer than those for the semi-taut and the catenary mooring systems, and the one for the catenary mooring system is the smallest. The reason is that the horizontal stiffness of the taut mooring system is a little smaller than that of the catenary and semi-taut mooring systems, which could be obtained from Figure 6. There are no significant changes in the natural periods of heave and pitch for the three cases, which means that the vertical stiffness of all the three cases is almost the same. With the increase of the water depth, the natural periods of surge increase a little, which is due to the increase of the added mass of the mooring line.

Table 5 **Natural periods**
Tablica 5 **Prirodni periodi**

Water depth (m)	Case	Surge (s)	Heave (s)	Pitch (s)
500	Catenary	180.4	34.5	81.9
	Semi-taut	211.6	34.5	82.5
	Taut	225.5	34.5	83.2
1000	Catenary	198.6	34.5	80.9
	Semi-taut	208.7	34.5	81.3
	Taut	228.5	34.5	82.5
1500	Catenary	208.8	34.5	78.9
	Semi-taut	241.6	34.5	79.5
	Taut	255.8	34.5	81.8

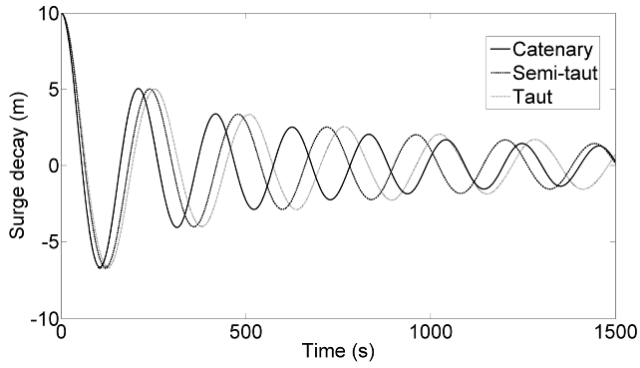

Figure 6(a) **Surge decay**
Slika 6(a) **Slobodno zalijetanje**

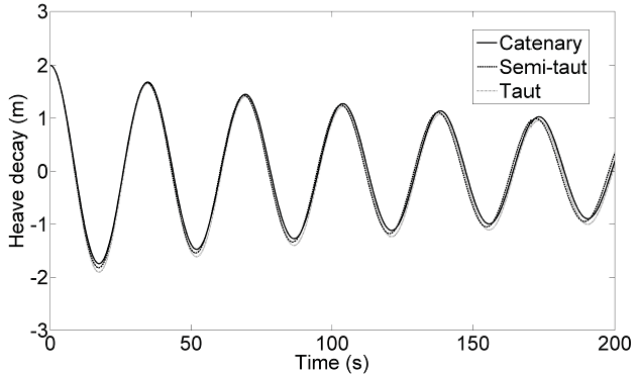

Figure 6(b) **Heave decay**
Slika 6(b) **Slobodno poniranje**

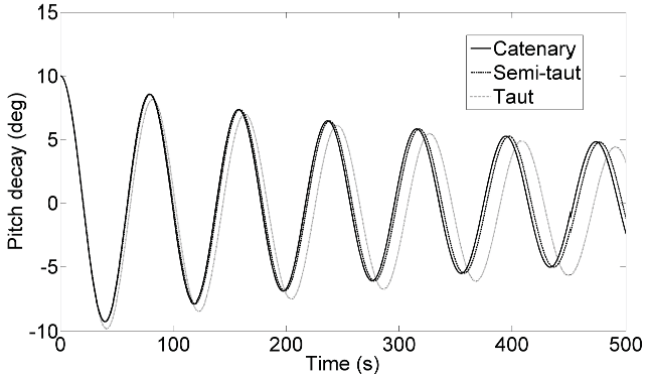

Figure 6(c) **Pitch decay**
Slika 6(c) **Slobodno posrtanje**

4.2 Damping ratios

The damping ratios derived from free decay simulations in 500 m, 1000 m and 1500 m water depths are summarized in Table 6. According to Table 6, the damping ratios of surge for the catenary mooring system are about 10% larger than those for the semi-taut system, and 20% larger than those for the taut mooring system. The reason is that the total length of the catenary mooring line is the largest, so the drag force in the catenary mooring line is the largest and the one of the semi-taut is in the second place. Therefore, the damping of the catenary mooring line is the largest. There is a little difference in the damping ratios of pitch for the three cases. The damping ratios of heave for the taut mooring system are the largest, and the ones for the catenary mooring system are the smallest. The reason is that the drag force along the mooring line in vertical direction is the largest in the taut mooring system due to the angle between the mooring line and the seabed. With the water depth increase, the natural damping ratios of surge increases and the one of heave decreases. The reason is that the pretension and stiffness of the three types of the mooring system in 500 m water depth is the smallest.

Table 6 **Damping ratios**
Tablica 6 **Omjeri prigušenja**

Water depth (m)	Case	Surge	Heave	Pitch
500	Catenary	4.60%	1.38%	2.08%
	Semi-taut	4.31%	1.56%	1.95%
	Taut	3.78%	2.25%	1.85%
1000	Catenary	5.13%	1.81%	2.06%
	Semi-taut	4.75%	2.06%	1.93%
	Taut	4.18%	2.85%	1.81%
1500	Catenary	5.36%	2.12%	2.13%
	Semi-taut	4.97%	2.36%	2.05%
	Taut	4.33%	3.05%	1.88%

4.3 Motion responses of DDMS platform

According to the calculation method on the spar platform above, the duration of 3 hours under a certain sea state conditions in the South China Sea is numerically simulated using the catenary, the semi-taut and the taut mooring systems. The statistics of the motions (surge, heave, and pitch) using the three types of the mooring systems in 500 m, 1000 m, and 1500 m water depths is summarized in Table 7. The motions time series and their spectra are plotted in Figures 7-12, and the ones in other water depths are omitted for the sake of conciseness. All spectra are smoothed by a 10-point averaging window.

Table 7 **Statistics of DDMS platform motions**
Tablica 7 **Statistika gibanja DDMS platforme**

Water depth = 500 m						
Motion		Average	σ	Max.	LF σ	WF σ
Surge (m)	Catenary	8.26	0.73	10.49	0.65	0.32
	Semi-taut	13.68	0.81	16.30	0.74	0.32
	Taut	15.99	0.81	18.60	0.74	0.32
Heave (m)	Catenary	-0.15	0.08	0.21	0.03	0.08
	Semi-taut	-0.13	0.08	0.15	0.03	0.08
	Taut	-0.09	0.08	0.12	0.03	0.08
Pitch (m)	Catenary	0.54	0.77	3.00	0.75	0.18
	Semi-taut	0.74	0.77	3.10	0.75	0.18
	Taut	0.84	0.80	3.15	0.78	0.18

Table 7. continued

Water depth = 1000 m						
Motion		Average	σ	Max.	LF σ	WF σ
Surge (m)	Catenary	9.31	0.76	11.77	0.69	0.32
	Semi-taut	12.53	0.87	15.31	0.82	0.32
	Taut	14.20	0.88	16.94	0.82	0.32
Heave (m)	Catenary	-0.18	0.08	0.21	0.03	0.08
	Semi-taut	-0.12	0.08	0.17	0.03	0.08
	Taut	-0.08	0.08	0.14	0.03	0.08
Pitch (m)	Catenary	0.44	0.70	2.78	0.72	0.18
	Semi-taut	0.75	0.74	3.06	0.72	0.18
	Taut	0.79	0.78	3.12	0.76	0.18
Water depth = 1500 m						
Motion		Average	σ	Max.	LF σ	WF σ
Surge (m)	Catenary	10.11	0.78	12.69	0.71	0.32
	Semi-taut	13.33	0.89	16.15	0.83	0.32
	Taut	14.65	0.91	17.50	0.85	0.32
Heave (m)	Catenary	-0.16	0.08	0.25	0.03	0.08
	Semi-taut	-0.06	0.08	0.20	0.03	0.08
	Taut	-0.04	0.08	0.14	0.03	0.08
Pitch (m)	Catenary	0.55	0.71	2.72	0.65	0.18
	Semi-taut	0.71	0.73	2.80	0.68	0.18
	Taut	0.74	0.76	2.89	0.74	0.18

Based on the results of the surge motions of the DDMS platform, the average, standard deviations and maximum surge motion for the three types of the mooring system is catenary < semi-taut < taut, and the results are similar to those for the natural damping ratios. In the LF range, the change laws of standard deviations of surge motion are the same as average surge motion which means that the LF motion dominates the total surge response. The efficient mooring line length of the catenary mooring system is the largest and the one of the taut mooring system is the smallest. Therefore, the mooring damping contribution of the catenary mooring system for the DDMS platform is the largest and the one of the taut mooring system is the smallest. In the WF range, the standard deviations of surge motion are same in the three cases. The reason is because the inertia forces in the WF range are dominant and the damping of the mooring lines does not make significant contributions to the reduction of the surge in the WF range. With the water depth increase, the average surge motion and standard deviations both increase, because the total mooring line length increases with the water depth.

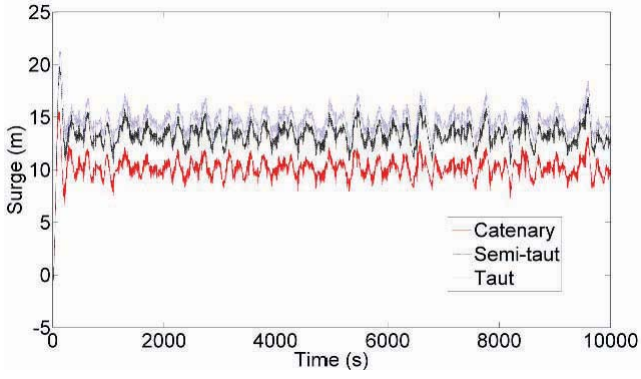

Figure 7 **Surge motions in 1500 m**
Slika 7 **Zalijetanje pri 1500 m dubine mora**

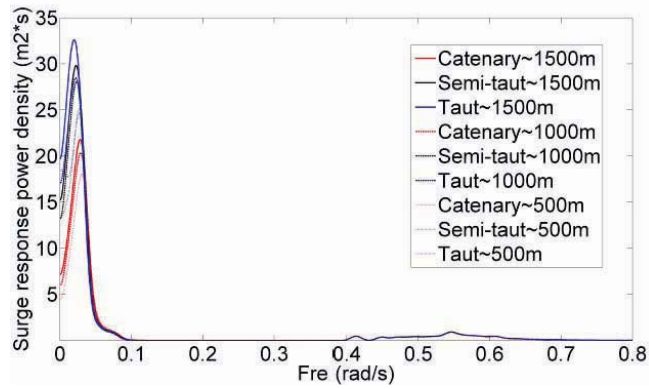

Figure 8 **Surge motions spectra**
Slika 8 **Spektar zalijetanja**

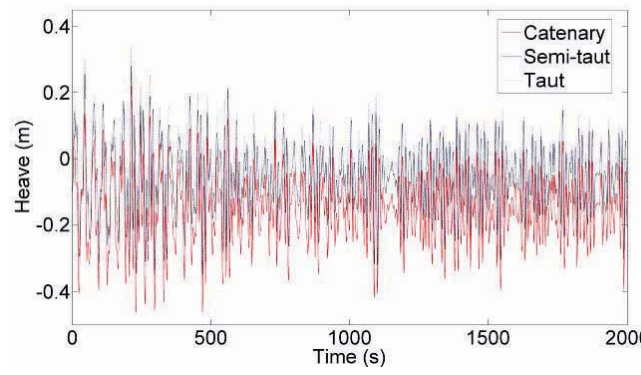

Figure 9 **Heave motions in 1500 m water depth**
Slika 9 **Poniranje pri dubini mora od 1500 m**

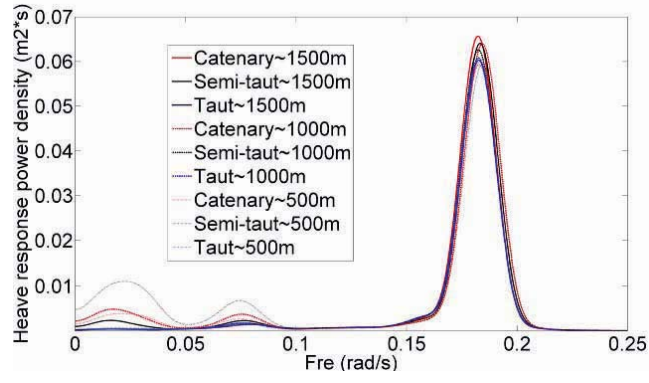

Figure 10(a) **Heave motions spectra (Fre<0.25)**
Slika 10(a) **Spektar poniranja, frekvencija manja od 0,25 rad/s**

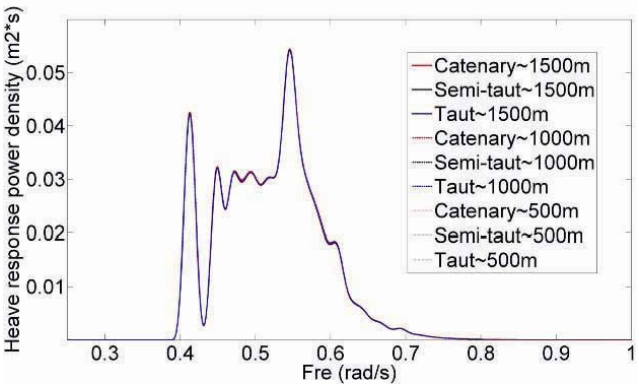

Figure 10(b) **Heave motions spectra (Fre>0.25)**
Slika 10(b) **Spektar poniranja, frekvencija veća od 0,25 rad/s**

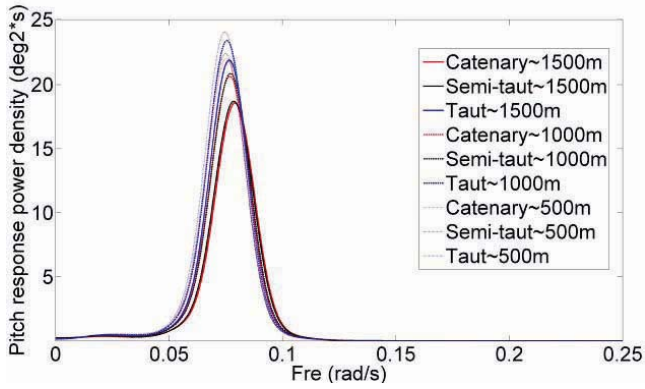

Figure 12(a) **Pitch motions spectra (Fre<0.25)**
Slika 12(a) **Spektar posrtanja, frekvencija manja od 0,25 rad/s**

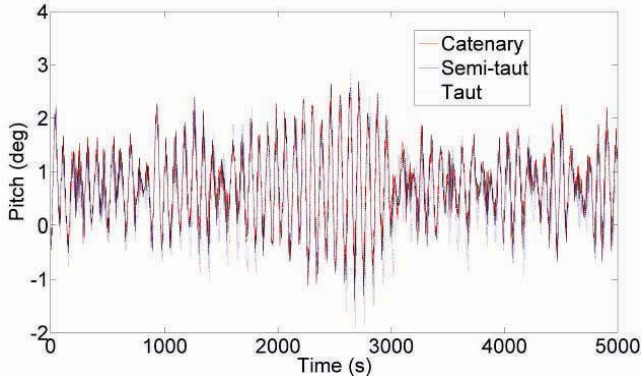

Figure 11 **Pitch motions in 1500 m water depth**
Slika 11 **Posrtanje pri dubini mora od 1500 m**

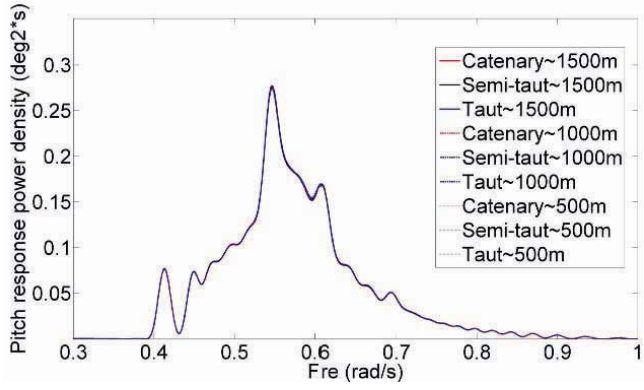

Figure 12(b) **Pitch motions spectra (Fre>0.25)**
Slika 12(b) **Spektar posrtanja, frekvencija veća od 0,25 rad/s**

Based on the results of the heave motions of the DDMS platform, the average and maximum heave motion for the three types of the mooring system is catenary > semi-taut > taut, and the WF motion dominates the total heave motion. This is because the mooring line length of the catenary mooring system is the largest, and the inertia force is the largest, the maximum heave motion of the catenary mooring system is the largest. With the water depth increase, the average and maximum heave motion both decrease due to the additional mooring damping. The standard deviations in the LF and WF range show insignificant changes, which means that heave responses are not sensitive to water depth changes.

Based on the results of the pitch motions of the DDMS platform, the average, standard deviations and maximum pitch motion for the three types of the mooring system is catenary < semi-taut < taut, which is the same as for the surge motion. In the LF and WF range, the change laws of the standard deviations of the pitch motion are also the same as for the surge motion due to similar reasons. With the water depth increase, the standard deviations in the WF range show insignificant change and the LF pitch motion slightly decreases, which means the mooring damping has a smaller effect on the LF pitch motion.

4.4 Mooring line tensions

With the same as motions responses of DDMS platform, two mooring lines are chosen to analyze: #1 is in downstream and the most unloaded mooring line, and #8 is in upstream and the most loaded mooring line. The statistics of the two mooring line tensions using the three types of the mooring systems in 500 m, 1000 m and 1500 m water depths are summarized in Table 8. The mooring line tensions time series and their spectra are plotted in Figures 13-15. All spectra are smoothed by a 10-point averaging window too.

Table 8 **Statistics of mooring line tensions**
Tablica 8 **Statistika vlačnih sila u sidrenoj liniji**

Water depth = 500 m								
Tension (kN)		Average	Average (Dynamic)	σ	Max.	Max. (Dynamic)	LF σ	WF σ
#1	Catenary	1080.2	80.2	12.7	1136.7	136.7	11.1	6.1
	Semi-taut	832.6	-67.4	6.1	856.8	-43.2	5.5	2.7
	Taut	790.2	-34.8	4.4	809.4	-15.6	3.9	1.9
#8	Catenary	1128.0	128.0	15.5	1184.3	184.3	14.3	7.5
	Semi-taut	1148.7	248.7	18.2	1207.2	307.2	16.2	8.3
	Taut	1135.1	310.1	26.2	1222.4	397.4	23.1	12.3
Water depth = 1000 m								
Tension (kN)		Average	Average (Dynamic)	σ	Max.	Max. (Dynamic)	LF σ	WF σ
#1	Catenary	1913.7	-86.3	11.0	1959.6	-40.4	9.8	5.1
	Semi-taut	1905.6	-44.4	9.4	1920.4	-29.6	8.5	3.9
	Taut	1633.1	-16.9	8.5	1661.5	11.5	7.7	3.6
#8	Catenary	2211.7	211.7	11.7	2257.2	257.2	10.6	4.9
	Semi-taut	2202.3	252.3	13.9	2240.4	290.4	12.2	6.5
	Taut	1989.6	339.6	19.4	2061.0	411.0	17.4	8.6
Water depth = 1500 m								
Tension (kN)		Average	Average (Dynamic)	σ	Max.	Max. (Dynamic)	LF σ	WF σ
#1	Catenary	2935.8	-64.2	11.3	3100.9	100.9	10.0	5.2
	Semi-taut	2947.8	47.8	9.5	2981.9	81.9	8.7	3.9
	Taut	2682.5	32.5	7.4	2710.8	60.8	6.7	3.0
#8	Catenary	3255.0	255.0	11.0	3294.7	294.7	10.0	4.5
	Semi-taut	3204.1	304.1	12.8	3238.9	338.9	11.3	4.9
	Taut	3025.2	375.2	13.7	3067.6	417.6	12.4	5.8

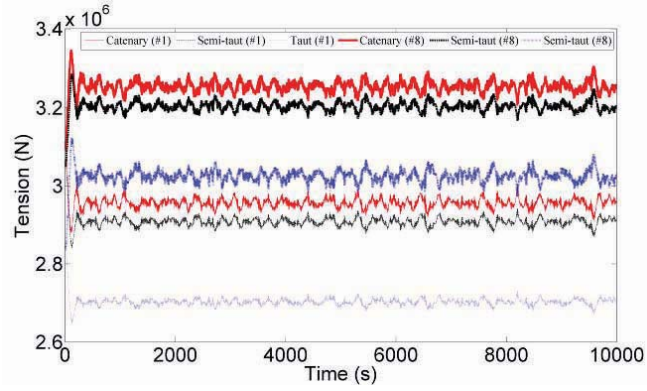

Figure 13 **Mooring line tension in 1500 m water depth**
Slika 13 **Vlačna sila u sidrenoj liniji pri dubini mora od 1500 m**

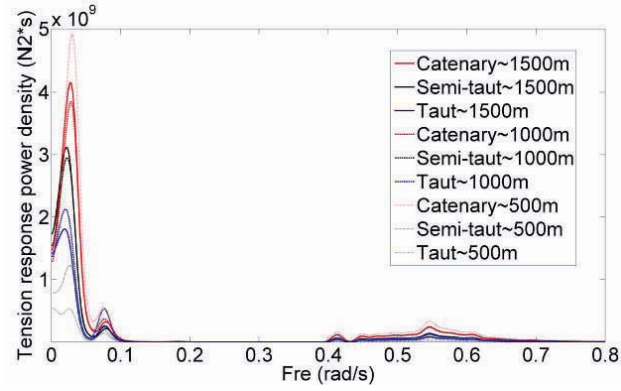

Figure 14 **Mooring line tension spectra of #1**
Slika 14 **Spektar vlačne sile u 1. sidrenoj liniji**

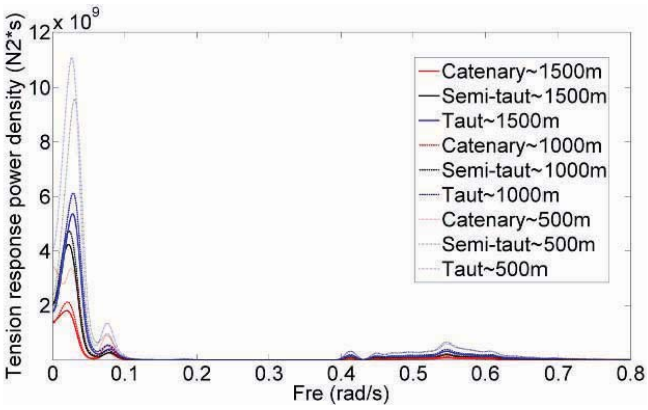

Figure 15 **Mooring line tension spectra of #8**
Slika 15 **Spektar vlačne sile u 8. sidrenoj liniji**

For the most unloaded mooring line #1, the dynamic mooring line tension is calculated through average mooring line tension minus their initial pretension. The change laws of both dynamic average and maximum mooring line tension are catenary > semi-taut > taut. The standard deviations in the LF and WF range for the three types of the mooring system is still catenary > semi-taut > taut. This phenomenon for the catenary mooring system is adverse and may cause more severe fatigue problem. For the most loaded mooring line #8, the change laws of average and standard deviations are just the opposite of #1.

The reason for different change laws between the mooring lines #1 and #8 is because the average tension of the mooring line #8 is much larger than in the case of the mooring line #1, which causes the mooring damping changes. According to investigation on the influence of pretension on mooring damping by Webster [29], the mooring damping increases with the amplitude of the motion if the pretension is smaller than the peak pretension, the mooring damping decreases with the amplitude of the motion if the pretension is larger than the peak pretension. Besides, the amplitudes of the motion responses of the DDMS using the taut mooring system are the largest. The average tension of #1 and #8 may just fall two sides of peak pretension, so the change laws are reasonable.

With the water depth increase, the dynamic mooring line tensions in both #1 and #8 decrease due to the increased mooring damping. The standard deviations in both the LF and WF range are the largest in 500 m water depth, which means the dynamic forces in the mooring lines become more significant when the length of the mooring lines becomes shorter. Therefore, the WF dynamic forces in the mooring lines are vital and should not be neglected in the simulation.

5 Conclusions

Through the comparison of the global responses of a DDMS platform and mooring line tensions using a catenary, a semi-taut and a taut mooring system in 500 m, 1000 m and 1500 m water depths in the South China Sea, the following preliminary findings are made:

- The natural periods of surge for the taut mooring system are longer than that for the semi-taut and catenary mooring systems, and the one for the catenary mooring system is the smallest. There are no significant changes in the natural periods of heave and pitch for the three considered cases. With the water depth increase, the natural periods of surge increase a little.
- The natural damping ratios are mainly determined by the efficient length of the mooring line. The natural damping ratios of surge for the catenary mooring system are about 10% larger than those for the semi-taut and 20% larger than those for the taut mooring system. There is a little difference in the natural damping ratios of pitch for the three cases. The natural damping ratios of heave for the taut mooring system are the largest. With the water depth increase, the natural damping ratios of surge increase and the one of heave decreases.
- The numerical simulation of the duration of three-hour simulation under certain sea state conditions reveals that the LF motion dominates the total surge and pitch motion. The WF motion dominates the total heave motion. With the water depth increase, both the average surge motion and standard deviations increase, both the average and maximum heave motion decrease, the standard deviations in the LF and WF range show insignificant changes, the standard deviations in the WF range show insignificant change, and the LF pitch motion slightly decreases.
- The DDMS platform using the catenary mooring system has the smallest surge and pitch motion, while the DDMS platform using the taut mooring system has the smallest heave motion.
- Only in the case of the mooring line tensions the obtained numerical simulation results are controversial. For the most unloaded mooring line, the taut mooring system is the most suitable because of its small amplitude changes. For the most loaded mooring line, the catenary mooring system is the most suitable because of its small extreme value.
- With the water depth increase, the dynamic mooring line tensions in mooring lines #1 and #8 decrease due to the increased mooring damping. The standard deviations in both the LF and WF range are the largest in 500 m water depth.

Acknowledgements

This paper is funded in part by the National Basic Research Program of China (Grant No. 2011CB013702; 2011CB013703), National Natural Science Foundation of China (Grant NO. 51209037; 50921001), China Postdoctoral Science Foundation Funded Project (Grant NO. 2012M510811), and the Fundamental Research Funds for the Central Universities (Grant No. DUT11RC(3)52).

References

[1] LIU, H. X., HUANG, Z. W.: "A New Type Deepwater Mooring System and Numerical Analytical Techniques", Ocean Technology, 26(2007), p. 6-10.
[2] DEVLIN, P., FLORY, J., HOMER, S.: "Deep Star Taut Leg Mooring Polyester Test Program", Oceans, Seattle, USA, (1999), p. 690-697.
[3] CHRISTIAN, A. C., SHANKAR, S. B.: "Fiber Mooring for Ultra-Deepwater Applications", Proceedings of the 12th International Offshore and Polar Engineering Conference, Kitatyusgu, Japan, (2002), p. 26-31.

[4] HUSE, E.: "Influence of Mooring Line Damping upon Rig Motions", Proceedings of the 18th Offshore Technology Conference, Houston, USA, (1986), p. 433-438.
[5] HUSE, E., MATSUMOTO, K.: "Practical Estimation of Mooring Line Damping", Proceedings of the 20th Offshore Technology Conference, Houston, USA, (1988), p. 543-552.
[6] WICHERS, J. E. W., HUIJISMANS, R. H. M.: "The Contribution of Hydrodynamic Damping Induced by Mooring Chains on Low Frequency Motions", Proceedings of the 22nd Offshore Technology Conference, Houston, USA, (1990), p. 171-182.
[7] CAO, P. M., ZHANG, J.: "Slow Motion Responses of Compliant Offshore Structures", International Journal of Offshore and Polar Engineering, 7(1997), p. 119-126.
[8] MA, W., LEE, M. Y., ZHOU, J., HUANG, E. W.: "Deepwater Nonlinear Coupled Analysis Tool", Proceedings of the 32nd Offshore Technology Conference, Houston, USA, (2000), No. OTC12085.
[9] TAHAR, A., RAN, Z., KIM, M. H.: "Hull/Mooring/Riser Coupled Spar Motion Analysis with Buoyancy-Can Effect", Proceedings of the 12th International Offshore and Polar Engineering Conference, Kitatyusgu, Japan, (2002), p. 223-230.
[10] LIU, T. J., CHEN, X. H., Wu, J. F., HUANG, K.: "Global Performance and Mooring Analysis of a Truss Spar", Proceedings of the 13th International Offshore and Polar Engineering Conference, Hawaii, USA, (2003), p. 256-263.
[11] KOO, B. J., KIM, M. H., RANDALL, R. E.: "The Effect of Nonlinear Multi-Contact Coupling with Gap Between Risers and Guide Frames on Global Spar Motion Analysis", Ocean Engineering, 31(2004), p. 1469-1502.
[12] LI, B. B., OU, J. P., TENG, B.: "Fully Coupled Effects of Hull, Mooring and Risers Model in Time Domain Based on an Innovative Deep Draft Multi-Spar", China Ocean Engineering, 24(2010), p. 219-233.
[13] CHEN, X. H., ZHANG, J., MA, W.: "On Dynamic Coupling Effects between a Spar and Its Mooring Lines", Ocean Engineering, 28(2001), p. 863-887.
[14] SHAFIEEFAR, M, REZVANI, A.: "Mooring Optimization of Floating Platforms Using a Genetic Algorithm", Ocean Engineering, 34(2007), p. 1413-1421.
[15] TONG, B., YANG, J. M., LI, X.: "Comparison and Analysis of Dynamic Effect for Mooring System of Semi-submerged Platform in Deep Water", The Ocean Engineering, 27(2009), p. 1-7.
[16] SUN, J. W., WANG, S. Q.: "Study on Motion Performance of Deepwater Spar Platform under Different Mooring Methods", Period of Ocean University of China, 40(2010), p. 147-153.
[17] LI, B. B., OU, J. P.: "Numerical Simulation on the Hydrodynamic and Kinetic Performance of a New Deep Draft Platform", Proceedings of the 19th International Offshore and Polar Engineering Conference, Osaka, Japan, (2009), p. 105-112.
[18] QIAO, D. S., OU, J. P.: "Static Analysis of a Deepwater Catenary Mooring System", Ship & Ocean Engineering, 38(2009), p. 120-124.
[19] SALVENSEN, N., TUCK, E. O., FALTINSEN, O.: "Ship Motions and Sea Loads", Trans. SNAME, 78(1970), p. 250-287.
[20] FALTINSEN, O. M.: "Sea Loads on Ships and Offshore Structures", Cambridge University Press, (1990), p. 37-54.
[21] GARRETT, D. L., CHAPPELL, J. F., GORDON, R. B.: "Global Performance of Floating Production Systems", Proceedings of the 34th Offshore Technology Conference, Houston, USA, (2002), No. OTC14230.
[22] PINKSTER, J. A.: "Mean and Low Frequency Wave Drifting Forces on Floating Structures", Ocean Engineering, 6(1979), p. 593-615.
[23] SUMER, B. M., FREDSØE, J.: "Hydrodynamics Around Cylindrical Structures", Advanced Series on Ocean Engineering, 26(2006), p. 131.
[24] PRISLIN, I., BLEVINS, R. D., HALKYARD, J. E.: "Viscous Damping and Added Mass of Solid Square Plates", Proceedings of the International Conference on Offshore Mechanics and Arctic Engineering, Lisbon, Portugal, (1998), No. 98-0316.
[25] GARRETT, D. L.: "Dynamic Analysis of Slender Rods", Journal of Energy Resources Technology, Trans. of ASME, 104(1982), p. 302-307.
[26] PAULLING, J. R., Webster, W. C.: "A Consistent Large-Amplitude Analysis of the Coupled Response of a TLP and Tendon System", Proceedings of the International Conference on Offshore Mechanics and Arctic Engineering, Tokyo, Japan, (1986), p. 126-133.
[27] NEWMAN, J. N.: "Marine Hydrodynamics", MIT Press, Cambridge, MA, (1978).
[28] CHEN, X. H., HUANG, K.: "Impacts of different riser models on global responses of a truss spar", Proceedings of International Symposium on Deepwater Mooring Systems, USA, (2003), p. 183-197.
[29] WEBSTER, W. C.: "Mooring-induced damping", Ocean Engineering, 22(1995), p. 571-591.